

Advances in the Mathematical Modelling of Hepatitis C Virus Dynamics

Narendra M. Dixit

Abstract | Mathematical models have provided key insights into the pathogenesis of hepatitis C virus (HCV) *in vivo*, suggested predominant mechanism(s) of drug action, explained confounding patterns of viral load changes in HCV infected patients undergoing therapy, and presented a framework for therapy optimization. In this article, I present an overview of the major advances in the mathematical modeling of HCV dynamics.

Introduction

Nearly 170 million people worldwide are infected with hepatitis C virus (HCV) [1]. Chronic HCV infection is a major cause of cirrhosis necessitating liver transplantation and often leading to death. The current treatment for HCV infection involves combination therapy with two drugs, pegylated interferon and ribavirin [2]. Combination therapy induces long-term responses in only ~50% of the patients treated [2,3]. For patients who do not respond to combination therapy, no effective alternatives exist [3]. It is of importance therefore to identify markers of disease progression and early predictors of therapeutic response that would suggest refinements of therapeutic protocols leading to enhancement of long-term response rates and/or minimization of exposure of patients to drugs, which remain expensive and have toxic side effects.

The responses of patients to combination therapy fall into three broad categories [4]. Sustained virological response (SVR) occurs when the concentration of viral particles in the blood, called viral load, falls below the detection limit (~100 HCV RNA copies per ml) during therapy and remains undetectable for 24 weeks after cessation of therapy. Patients exhibiting SVR are generally cured of the infection. In some patients, the viral load becomes undetectable during therapy, called an end-of-treatment response (ETR), but relapses upon cessation of therapy. Reinstatement of therapy may

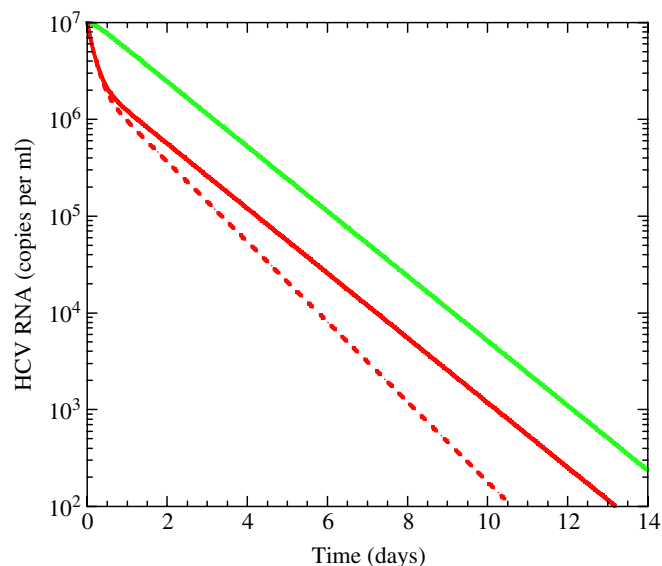
lead to SVR in such patients. In some patients, called non-responders, the viral load remains detectable throughout. Upon initiation of therapy, such patients experience either an initial drop in the viral load followed by a nearly constant detectable viral load (flat response) or no drop at all (null response).

The profiles of viral load decline in patients following the initiation of therapy serve as broad indicators of long-term response [4]. The pretreatment viral load remains approximately constant in chronically infected patients. Following the onset of therapy, the viral load drops in a biphasic or triphasic manner. In responders with a biphasic decay pattern, a sharp drop occurs for the first 1–2 days, followed by a slower second phase decline until viral load becomes undetectable. In patients exhibiting a transient response followed by relapse, the initial drop and/or the second phase decline may be subdued. Non-responders typically do not exhibit a significant second phase decline. When a triphasic response is observed, a shoulder phase of 4–28 days duration, where the viral load is nearly constant, separates the initial sharp drop and the subsequent slow decline [5].

These intriguing patterns of viral load changes in HCV infected patients under therapy hold clues to HCV pathogenesis *in vivo* and outcomes of therapy. Over the past decade, mathematical models of HCV dynamics have been developed that have

*Department of Chemical Engineering, and Bioinformatics Center, Supercomputer Education and Research Center, Indian Institute of Science, Bangalore 560012
narendra@chemeng.iisc.ernet.in*

Figure 1: Decline in viral load following the onset of therapy predicted by Eqs. (2) and (3) with $\eta=0.8, \varepsilon=0$ (green); $\eta=0, \varepsilon=0.8$ (red solid); $\eta=0.8, \varepsilon=0.8$ (red dashed). The uninfected cell density is held constant at the pretreatment value $T = c\delta/p\beta$. The initial viral load, $V_0 = 10^7$ copies ml⁻¹, and the infected cell density, $I_0 = cV_0/p$. Parameter values employed are $\beta = 2.25 \times 10^{-7}$ ml day⁻¹ virions⁻¹, $\delta = 1$ day⁻¹, $p = 2.9$ virions cell⁻¹ day⁻¹, and $c = 6$ day⁻¹.



gradually unraveled the origins of these patterns. Below, I present a brief account of the models that have resulted in significant advances in our understanding of HCV dynamics.

Basic model of HCV dynamics

Following the success of models of the dynamics of human immunodeficiency virus (HIV) [6,7] and hepatitis B virus infections [8], Neumann et al [9] adapted the basic model of viral dynamics to HCV. The model assumes a simplified view of HCV infection and describes the response to interferon therapy through the coupled evolution of three populations, viz., uninfected hepatocytes, productively infected hepatocytes, and free HCV virions, with the following equations.

$$\frac{dT}{dt} = s - dT - (1 - \eta)\beta VT \quad (1)$$

$$\frac{dI}{dt} = (1 - \eta)\beta VT - \delta I \quad (2)$$

$$\frac{dV}{dt} = (1 - \varepsilon)pI - cV \quad (3)$$

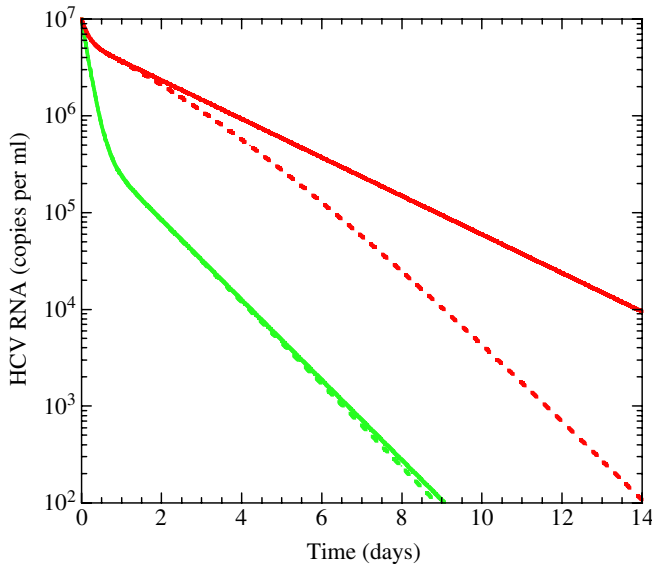
Here, uninfected hepatocytes, T , are produced at rate s and die with first order rate constant d . Free virions, V , infect uninfected hepatocytes at rate βVT and produce productively infected

hepatocytes, I . Infected hepatocytes are lost, primarily due to immune mediated killing, at rate δ . Free virions are produced at rate p per infected hepatocyte and are cleared from circulation at rate c . Two possible mechanisms of interferon action are assumed. Interferon could block de novo infection of cells with effectiveness η or lower viral production from infected cells with effectiveness ε .

Before treatment, $\eta = \varepsilon = 0$ and a steady state exists where viral production is balanced by viral clearance and the production of infected cells is balanced by their loss. Uninfected hepatocytes are also in steady state determined by the balance between their production, death, and loss due to infection. Following the onset of therapy, at time $t = 0$, I and V decline and T increases due to drug action. Interestingly, V decays in a single (exponential) phase with time if $\varepsilon = 0$ and $\eta > 0$, whereas if $0 < \varepsilon < 1$ the decay occurs in two distinct phases (Fig. 1). Further, when $0 < \varepsilon < 1$, the decay is influenced negligibly by changes in η . Because experimental data of viral load changes in patients is inconsistent with a single phase decay, Neumann et al [9] concluded that interferon acts against HCV by lowering the production and/or release of new virions from infected cells. The effect of interferon in blocking de novo infections is negligible. Indeed, in vitro experiments confirmed that interferon blocks viral production from infected cells [10].

With $\eta = 0$, Neumann et al [9] compared model predictions with experimental measurements of viral load changes in patients following the onset of therapy. For the short periods under therapy (up to 14 days), when viral load measurements were analyzed, the uninfected hepatocyte numbers may be assumed to remain constant. Typically, viral clearance and production are rapid compared to the formation and loss of infected cells. Immediately upon the onset of therapy, after a small pharmacokinetic delay, viral production is lowered from the pretreatment value due to drug action. During this period, with the assumption that changes in the infected cell numbers are small, Eqs. (1)–(3) predict that V declines exponentially with the characteristic timescale $1/c$ and reaches the asymptotic value $V_0(1 - \varepsilon)$, where V_0 is the pretreatment viral load. This marks the first phase of viral load decline. The lower viral load achieved in the first phase decreases the formation of new infected cells. The resulting imbalance in the production and loss rates of infected cells causes a decline in I . During this period, viral production and clearance remain in pseudo steady state and V declines in proportion to I . Using the pseudo-steady state approximation, Eqs. (1)–(3) predict an exponential decline of V with a characteristic

Figure 2: Decline in viral load following the onset of therapy predicted by Eqs. (5)–(7) with $\varepsilon = 0.96$ (green) and 0.5 (red) and $\rho_{\max} = 0$ (solid) and 1 (dashed). The uninfected cell density is held constant at the pretreatment value $T = c\delta/p\beta$. The initial viral load, $V_0 = 10^7$ copies ml^{-1} , and the infected cell density, $I_0 = cV_0/p$. The slow accumulation of ribavirin is approximated using $\rho = \rho_{\max}(1 - \exp(-t/t_a))$. Parameter values employed are $\beta = 2.25 \times 10^{-7}$ ml day^{-1} virions^{-1} , $\delta = 1$ day^{-1} , $p = 2.9$ virions cell^{-1} day^{-1} , $c = 6$ day^{-1} , and $t_a = 5.6$ days.



timescale that depends on ε , δ and c . This marks the second phase of viral load decline.

The basic model thus explains the origins of the biphasic decline in viral load following the onset of interferon therapy. Model predictions provide good fits to experimental data and yield estimates of model parameters that determine key characteristics of HCV pathogenesis in vivo and the effectiveness of therapy [9]. From the extent and the rate of viral load decline in the first phase, the parameters ε and c , respectively, were obtained. The slope of the second phase decline then allowed estimation of δ . The virion half-life was thus estimated to be ~ 2.7 hours suggesting a massive pretreatment production of $\sim 10^{12}$ virions per day in a chronically infected individual. Estimates of the infected cell life-span exhibited large variations, from 1.7–70 days. Further, the interferon effectiveness was estimated to be high and increased from $\sim 80\%$ to $\sim 96\%$ as the daily dosage of interferon was varied from 5 to 15 million international units.

The basic model thus provides key insights into HCV dynamics in vivo. In addition, the model enables comparisons of the in vivo effectiveness of alternative therapies [9,11,12], which facilitates the identification of improved protocols. The model, however, is unable to predict the long-term response rates observed during combination therapy because it ignores the influence of ribavirin.

The influence of ribavirin

The addition of ribavirin to interferon therapy significantly improves long-term response rates [2]. For instance, following 48 weeks of interferon therapy, the percentage of patients treated who exhibited SVR increased from $\sim 13\%$ without to $\sim 38\%$ with ribavirin [13]. Ribavirin alone, however, induced short-term transient declines in viral load in some patients [14], but no long-term responses [15,16]. To understand the role of ribavirin in interferon therapy, Dixit et al. [17] advance the basic model to explicitly include ribavirin action. The mechanism of ribavirin action against HCV remains poorly established [18,19]. Of the several possibilities, the predominant mechanism is thought to be mutagenesis. Ribavirin, a guanosine analog, gets incorporated in replicating viral RNA strands and increases the viral mutation rate [20]. The large mutation rate may compromise the ability of progeny virions to infect cells and/or replicate [21,22]. Dixit et al. [17] assume that ribavirin renders a fraction, ρ , of progeny virions non-infectious and write

$$\frac{dT}{dt} = s - dT - \beta V_I T \quad (4)$$

$$\frac{dI}{dt} = \beta V_I T - \delta I \quad (5)$$

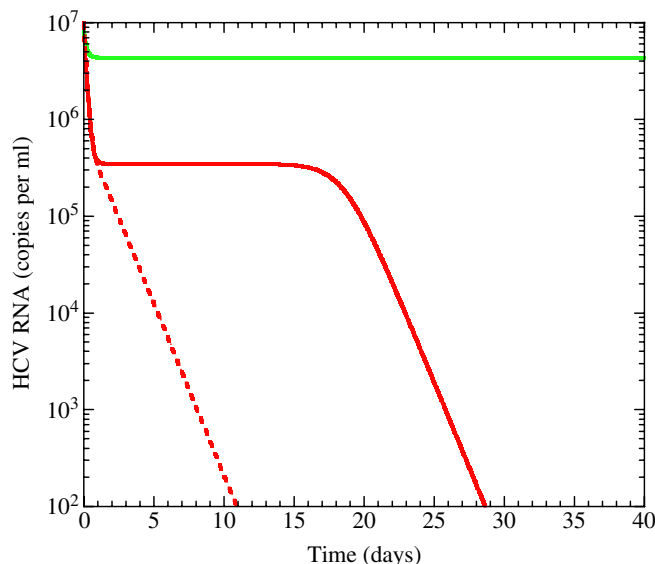
$$\frac{dV_I}{dt} = (1 - \rho)(1 - \varepsilon)pI - cV_I \quad (6)$$

$$\frac{dV_{NI}}{dt} = \rho(1 - \varepsilon)pI - cV_{NI} \quad (7)$$

Here, the viral load V is partitioned into infectious virions, V_I , and non-infectious virions, V_{NI} . Assuming again that the uninfected hepatocyte population remains at the pretreatment value, Dixit et al. [17] solved the above equations and predicted changes in V in patients undergoing combination therapy.

Interestingly, model predictions suggest that ribavirin does not alter the first phase decline induced by interferon. Further, when interferon effectiveness is large, $\varepsilon \sim 1$, ribavirin does not alter significantly the second phase decline either. When ε is significantly smaller than 1, ribavirin enhances the second phase slope (Fig. 2). The enhancement is proportional to the ribavirin effectiveness ρ and increases as ε is decreased. These intriguing effects of ribavirin in combination therapy may be understood as follows. The first phase decline is a consequence of the imbalance between viral production and clearance caused by interferon. Because ribavirin does not alter viral production, it has no influence on the first phase decline. By

Figure 3: Decline in viral load following the onset of therapy predicted by Eqs. (8)–(11) with $r_I = r_T = 2 \text{ day}^{-1}$, $\varepsilon = 0.5$ (green) and 0.96 (red solid), and $5r_I = r_T = 10 \text{ day}^{-1}$, $\varepsilon = 0.96$ (red dashed). The initial conditions are determined from the pretreatment steady state. Parameter values employed are $\beta = 2.25 \times 10^{-7} \text{ ml day}^{-1} \text{ virions}^{-1}$, $\delta = 1 \text{ day}^{-1}$, $p = 2.9 \text{ virions cell}^{-1} \text{ day}^{-1}$, $c = 6 \text{ day}^{-1}$, $s = 1 \text{ cells ml}^{-1} \text{ day}^{-1}$, $d = 0.01 \text{ day}^{-1}$, $T_{\max} = 3.6 \times 10^7 \text{ cells ml}^{-1}$, and $\rho = 0$. The critical efficacy for these parameter values is $\varepsilon_c \sim 0.75$.



rendering a fraction of virions produced non-infectious, ribavirin lowers the rate at which new infected cells are produced. When interferon effectiveness is large, viral production is so low that ribavirin has little role to play. When interferon effectiveness is small, ribavirin renders progeny virions non-infectious and enhances the second phase decline. Indeed, experimental observations confirm that ribavirin does not influence the first phase slope and enhances the second phase slope when interferon effectiveness is small [14,23,24]. The above model thus reconciles the seemingly conflicting observations that ribavirin enhances the second phase slope under some circumstances and not in others.

The model also suggests that the immunomodulatory effect of ribavirin, which is considered a possible alternative mechanism of ribavirin action against HCV [18,19], does not play a major antiviral role. By enhancing the immune response against HCV, *i.e.*, by increasing the loss rate of infected cells δ , ribavirin would increase the second phase slope regardless of interferon effectiveness. In contrast, ribavirin enhances the second phase slope when interferon effectiveness is small, as observed in experiments.

More importantly, the model explains the enhancements in long-term response rates in

patients induced by ribavirin [13,25–27]. Model predictions capture experimental viral load changes in patients quantitatively and provide refined estimates of model parameters. In particular, the comparisons identify the mean and the distribution of the loss rate of infected cells δ among patients. Because the second phase slope depends on both the effectiveness of therapy and the strength of the immune response, the model predicts threshold values of δ , called δ_{SVR} and δ_{ETR} , required for viral eradication and suppression below detection, respectively, for given values of drug effectiveness and duration of therapy. Patients with $\delta > \delta_{SVR}$ (δ_{ETR}) achieve SVR (ETR). From the distribution of δ among patients, and with the mean effectiveness of interferon and ribavirin, the model predicts the fraction of patients that would exhibit SVR without and with ribavirin. Remarkably, model predictions are in close agreement with experiments [17,19]. An understanding of the role of ribavirin in the long-term outcome of therapy thus emerges. Besides, by explicitly accounting for ribavirin action, the model presents a framework for optimization of combination therapy.

The role of liver homeostatic mechanisms

A key limitation of the model of Dixit et al. [17] is its restriction to biphasic responses; non-responders and patients with triphasic decay patterns are not described. In a recent study, Dahari et al. [28,29] advance the model of Dixit et al. [17] to include proliferation of uninfected and infected cells driven by liver homeostatic mechanisms and predict the triphasic decline and explain the origins of non-response. The model equations are

$$\frac{dT}{dt} = s + r_T \left(1 - \frac{T+I}{T_{\max}}\right) - dT - \beta V_I T \quad (8)$$

$$\frac{dI}{dt} = \beta V_I T + r_I \left(1 - \frac{T+I}{T_{\max}}\right) - \delta I \quad (9)$$

$$\frac{dV_I}{dt} = (1 - \rho)(1 - \varepsilon)pI - cV_I \quad (10)$$

$$\frac{dV_{NI}}{dt} = \rho(1 - \varepsilon)pI - cV_{NI} \quad (11)$$

Here, uninfected cells proliferate at maximum rate r_T and infected cells at maximum rate r_I . The total number of hepatocytes, $T + I$, can attain the maximum value T_{\max} , at which point cell proliferation stops. The remaining terms in Eqs. (8)–(11) are identical to those in Eqs. (4)–(7).

The model of Dahari et al. [29] makes two important predictions. First, the model predicts the existence of a critical effectiveness of therapy below which therapy cannot induce long-term viral

load decline (Fig. 1C). Eqs. (8)–(11) have two steady states: the uninfected steady state where $V = I = 0$ and an infected steady state obtained by setting the right hand sides of Eqs. (8)–(11) to zero. From the latter steady state, a critical effectiveness of therapy can be determined below which the viral load reaches a new (lower) steady state under therapy. This describes the viral decay profiles exhibited by non-responders. The critical effectiveness depends both on viral and host factors and the same therapy may be below or above the critical effectiveness in different patients. When the effectiveness is above the critical value, viral load declines continuously during therapy and results in long-term response.

The second key prediction of the model is that the decline in viral load, when the effectiveness of therapy is above the critical value, can be either biphasic or triphasic (Fig. 3). The triphasic decline emerges as a consequence of homeostatic cell proliferation. During the first phase, viral production drops due to interferon action and the viral load decreases. Consequently, the production of infected cells by new infections decreases and the total number of cells falls. Homeostatic mechanisms act to restore the total cell number by cell proliferation. Because both uninfected and infected cells can proliferate, when the number of uninfected cells is small, homeostatic mechanisms result predominantly in the proliferation of infected cells. A new steady state is reached where the production of infected cells by new infections and proliferation is balanced by infected cell loss due to immune mediated killing. Accordingly, the viral load, which is in pseudo equilibrium with the infected cell population, also reaches a plateau. This marks the shoulder phase of the triphasic decline. During this interim steady state, however, the total cell number is smaller than the maximum value, T_{\max} , and the proliferation of uninfected cells continues. When the uninfected cell number becomes comparable to that of infected cells, the loss of infected cells is compensated for by the proliferation of uninfected cells. The number of infected cells then declines and the viral load drops marking the onset of the third phase of viral load decline. When the number of infected cells during the chronic infection steady state is small compared to the number of uninfected cells, the shoulder phase does not occur and a biphasic response is observed.

The model thus explains the various viral load decay profiles observed in patients undergoing combination therapy. Model predictions are able to capture experimental viral load changes in patients quantitatively [29]. The model suggests further that the slow second phase decline (or plateau)

observed in patients does not imply a small loss rate of infected cells. Instead, the slope of the third phase decline is indicative of the loss rate of infected cells. The large range of values of δ estimated by Neumann et al. [9] is thus an overestimate of the variance of the infected cell lifespan across patients. Obtaining refined estimates of model parameters using the model of Dahari et al. [29], however, remains difficult because the model introduces additional unknown parameters describing liver homeostatic mechanisms. Future experiments may provide information on liver homeostatic mechanisms and hepatocyte populations that would facilitate the application of the model to the systematic analysis of viral load changes in patients.

Concluding remarks

Models of HCV dynamics provide key insights into HCV pathogenesis in vivo and the mechanisms of action of interferon and ribavirin against HCV [30]. The models elucidate the origins of different viral load decay patterns observed in patients, make predictions of the long-term outcomes of therapy, and present a framework for rational therapy optimization. A few pieces of the puzzle, however, are still missing.

First, therapy optimization hinges on accurate descriptions of drug pharmacokinetics. Models of HCV dynamics that incorporate the pharmacokinetics of interferon have been suggested [31]. The pharmacokinetics of ribavirin, which exhibits an unusual three phase plasma concentration-time profile, however, remains poorly described [32]. Second, current HCV models assume ribavirin action to render a fraction of virions noninfectious, due possibly to mutagenesis. Although recent reports provide increasing evidence of the enhancement of the HCV mutation rate by ribavirin, the evidence is still not conclusive [33,34]. Establishment of the mechanism of ribavirin action is critical to understanding several aspects of HCV dynamics. Current models, for instance, are unable to explain the transient viral load decline observed in some patients during ribavirin monotherapy [14]. Ribavirin alone does not induce long-term responses but enhances significantly response rates in combination with interferon suggesting that ribavirin and interferon act synergistically in vivo. The origins of the synergy remain poorly understood [35]. Indeed, recent models that present detailed descriptions of the intracellular events of the HCV lifecycle [36] would aid the development of fundamental descriptions of drug action. Third, quantitative descriptions of the side effects of drugs, e.g., hemolytic anemia induced by ribavirin [37], which limit dosages and constrain

therapy optimization, are currently lacking. Finally, robust links between long-term response to therapy and markers of disease state such as viral load and alanine aminotransferase levels [38,39] are yet to be established. Disease progression depends not only on viral and drug characteristics but also on host genetic factors, which remain difficult to determine. Accurate, early predictors of long-term response will facilitate personalization of therapy and substantially improve our ability to combat the HCV pandemic.

Acknowledgement

This work was supported by the Centre of Excellence for Research on Hepatitis C Virus, Department of Biotechnology, India.

Received 11 March 2008; revised 07 April 2008.

References

- World Health Organization (2000) Hepatitis C - global prevalence (update). *World Health Org Weekly Epidemiol Rec* 75: 18–19.
- National Institutes of Health (2002) Consensus statement on management of hepatitis C. *NIH Consens State Sci Statements* 19: 1–46.
- Tan SL, Pause A, Shi Y, Sonenberg N (2002) Hepatitis C therapeutics: Current status and emerging strategies. *Nature Rev Drug Discov* 1: 867–881.
- Feld JJ, Hoofnagle JH (2005) Mechanism of action of interferon and ribavirin in treatment of hepatitis C. *Nature* 436: 967–972.
- Herrmann E, Lee JH, Marinos G, Modi M, Zeuzem S (2003) Effect of ribavirin on hepatitis C viral kinetics in patients treated with pegylated interferon. *Hepatology* 37: 1351–1358.
- Perelson AS, Neumann AU, Markowitz M, Leonard JM, Ho DD (1996) HIV-1 dynamics in vivo: Virion clearance rate, infected cell life-span, and viral generation time. *Science* 271: 1582–1586.
- Wei XP, Ghosh SK, Taylor ME, Johnson VA, Emimi EA, et al. (1995) Viral Dynamics in Human-Immunodeficiency-Virus Type-1 Infection. *Nature* 373: 117–122.
- Nowak MA, Bonhoeffer S, Hill AM, Boehme R, Thomas HC, et al. (1996) Viral dynamics in hepatitis B virus infection. *Proc Natl Acad Sci USA* 93: 4398–4402.
- Neumann AU, Lam NP, Dahari H, Gretch DR, Wiley TE, et al. (1998) Hepatitis C viral dynamics in vivo and the antiviral efficacy of interferon- α therapy. *Science* 282: 103–107.
- Chung RT, He WP, Saquib A, Contreras AM, Xavier RJ, et al. (2001) Hepatitis C virus replication is directly inhibited by IFN- α in a full-length binary expression system. *Proc Natl Acad Sci USA* 98: 9847–9852.
- Neumann AU, Lam NP, Dahari H, Davidian M, Wiley TE, et al. (2000) Differences in viral dynamics between genotypes 1 and 2 of hepatitis C virus. *J Infect Dis* 182: 28–35.
- Zeuzem S, Herrmann E, Lee JH, Fricke J, Neumann AU, et al. (2001) Viral kinetics in patients with chronic hepatitis C treated with standard or peginterferon alpha 2a. *Gastroenterology* 120: 1438–1447.
- McHutchison JG, Gordon SC, Schiff ER, Shiffman ML, Lee WM, et al. (1998) Interferon α -2b alone or in combination with ribavirin as initial treatment for chronic hepatitis C. *N Engl J Med* 339: 1485–1492.
- Pawlotsky JM, Dahari H, Neumann AU, Hezode C, Germanidis G, et al. (2004) Antiviral action of ribavirin in chronic hepatitis C. *Gastroenterology* 126: 703–714.
- Dusheiko G, Main J, Thomas H, Reichard O, Lee C, et al. (1996) Ribavirin treatment for patients with chronic hepatitis C: results of a placebo-controlled study. *J Hepatol* 25: 591–598.
- Zoulim F, Haem J, Ahmed S S, Chossegros P, Habersetzer F, et al. (1998) Ribavirin monotherapy in patients with chronic hepatitis C: a retrospective study of 95 patients. *J Viral Hepat* 5: 193–198.
- Dixit NM, Layden-Almer JE, Layden TJ, Perelson AS (2004) Modelling how ribavirin improves interferon response rates in hepatitis C virus infection. *Nature* 432: 922–924.
- Lau JYN, Tam RC, Liang TJ, Hong Z (2002) Mechanism of action of ribavirin in the combination treatment of chronic HCV infection. *Hepatology* 35: 1002–1009.
- Dixit NM, Perelson AS (2006) The metabolism, pharmacokinetics and mechanisms of antiviral activity of ribavirin against hepatitis C virus. *Cell Mol Life Sci* 63: 832–842.
- Crotty S, Cameron CE, Andino R (2001) RNA virus error catastrophe: Direct molecular test by using ribavirin. *Proc Natl Acad Sci USA* 98: 6895–6900.
- Lanford RE, Guerra B, Lee H, Averett DR, Pfeiffer B, et al. (2003) Antiviral effect and virus-host interactions in response to alpha interferon, gamma interferon, poly(I)-poly(C), tumor necrosis factor alpha, and ribavirin in hepatitis C virus subgenomic replicons. *J Virol* 77: 1092–1104.
- Zhou SF, Liu R, Baroudy BM, Malcolm BA, Reyes GR (2003) The effect of ribavirin and IMPDH inhibitors on hepatitis C virus subgenomic replicon RNA. *Virology* 310: 333–342.
- Herrmann E, Lee JH, Marison G, Modi M, Zeuzem S (2003) Effect of ribavirin on hepatitis C viral kinetics in patients treated with pegylated interferon. *Hepatology* 37: 1351–1358.
- Layden-Almer JE, Ribeiro RM, Wiley T, Perelson AS, Layden TJ (2003) Viral dynamics and response differences in HCV-infected African American and white patients treated with IFN and ribavirin. *Hepatology* 37: 1343–1350.
- Fried MW, Shiffman ML, Reddy KR, Smith C, Marinos G, et al. (2002) Peginterferon alfa-2a plus ribavirin for chronic hepatitis C virus infection. *N Engl J Med* 347: 975–982.
- Poynard T, Marcellin P, Lee SS, Niederau C, Minuk GS, et al. (1998) Randomized trial of interferon α 2b plus ribavirin for 48 weeks or for 24 weeks versus interferon α 2b plus placebo for 48 weeks for treatment of chronic infection with hepatitis C virus. *Lancet* 352: 1426–1432.
- Reichard O, Norrkranz G, Frydén A, Braconier JH, Sönnberg A, et al. (1998) Randomized, double-blind, placebo-controlled trial of interferon α -2b with and without ribavirin for chronic hepatitis C. *Lancet* 351: 83–87.
- Dahari H, Lo A, Ribeiro RM, Perelson AS (2007) Modeling hepatitis C virus dynamics: Liver regeneration and critical drug efficacy. *J Theor Biol* 247: 371–381.
- Dahari H, Ribeiro RM, Perelson AS (2007) Triphasic decline of hepatitis C virus RNA during antiviral therapy. *Hepatology* 46: 16–21.
- Perelson AS, Herrmann E, Micol F, Zeuzem S (2005) New kinetic models for the hepatitis C virus. *Hepatology* 42: 749–754.
- Powers KA, Dixit NM, Ribeiro RM, Golia P, Talal AH, et al. (2003) Modeling viral and drug kinetics: hepatitis C virus treatment with pegylated interferon α -2b. *Semin Liv Dis* 23: 13–18.
- Glue P (1999) The clinical pharmacology of ribavirin. *Semin Liv Dis* 19: 17–24.
- Perelson AS, Layden TJ (2007) Ribavirin: Is it a mutagen for hepatitis C virus? *Gastroenterology* 132: 2050–2052.
- Chevaliez S, Brillet R, Lazaro E, Hezode C, Pawlotsky JM (2007) Analysis of ribavirin mutagenicity in human hepatitis C virus infection. *J Virol* 81: 7732–7741.
- Zhang YH, Jamaluddin M, Wang SF, Tian B, Garofalo RP, et al. (2003) Ribavirin treatment up-regulates antiviral gene

- expression via the interferon-stimulated response element in respiratory syncytial virus-infected epithelial cells. *J Virol* 77: 5933–5947.
36. Dahari H, Ribeiro RM, Rice CM, Perelson AS (2007) Mathematical modeling of subgenomic hepatitis C virus replication in Huh-7 cells. *J Virol* 81: 750–760.
 37. De Franceschi L, Fattovich G, Turrini F, Ayi K, Brugnara C, et al. (2000) Hemolytic anemia induced by ribavirin therapy in patients with chronic hepatitis C virus infection: Role of membrane oxidative damage. *Hepatology* 31: 997–1004.
 38. Ribeiro RM, Layden-Almer J, Powers KA, Layden TJ, Perelson AS (2003) Dynamics of alanine aminotransferase during hepatitis C virus treatment. *Hepatology* 38: 509–517.
 39. Colombatto P, Civitano L, Oliveri F, Coco B, Ciccorossi P, et al. (2003) Sustained response to interferon-ribavirin

combination therapy predicted by a model of hepatitis C virus dynamics using both HCV RNA and alanine aminotransferase. *Antivir Ther* 8: 519–530.



Narendra M. Dixit holds a bachelors degree from IIT Bombay and masters and doctoral degrees from the University of Illinois at Urbana-Champaign, all in chemical engineering. Following postdoctoral studies at the Los Alamos National Laboratory in theoretical biology and biophysics, he now serves on the faculty of the Indian Institute of Science.